

Evidence for a new ^{12}C state at 13.3 MeV

M. Freer,¹ S. Almaraz-Calderon,² A. Aprahamian,² N. I. Ashwood,¹ M. Barr,¹ B. Bucher,² P. Copp,³ M. Couder,² N. Curtis,¹ X. Fang,² F. Jung,² S. Leshner,³ W. Lu,² J. D. Malcolm,¹ A. Roberts,² W. P. Tan,² C. Wheldon,¹ and V. A. Ziman¹

¹*School of Physics and Astronomy, University of Birmingham, Birmingham B15 2TT, United Kingdom*

²*Institute for Structure and Nuclear Astrophysics, Department of Physics, University of Notre Dame, Notre Dame, Indiana 46556, USA*

³*Department of Physics, University of Wisconsin–La Crosse, La Crosse, Wisconsin 54601, USA*

(Received 13 January 2011; revised manuscript received 4 February 2011; published 15 March 2011)

The two reactions $^{12}\text{C}(^4\text{He}, ^4\text{He} + ^4\text{He})^4\text{He}$ and $^9\text{Be}(^4\text{He}, ^4\text{He} + ^4\text{He} + ^4\text{He})n$ were measured using an array of four double-sided strip detectors. Excited states in ^{12}C were reconstructed filtered by the condition that the α -decay proceeded via the ^8Be ground state. In both measurements, evidence was found for a new state at 13.3(0.2) MeV with a width 1.7(0.2) MeV. Angular correlation measurements from the $^{12}\text{C}(^4\text{He}, ^4\text{He} + ^4\text{He} + ^4\text{He})^4\text{He}$ reaction indicates that the state may have $J^\pi = 4^+$.

DOI: [10.1103/PhysRevC.83.034314](https://doi.org/10.1103/PhysRevC.83.034314)

PACS number(s): 21.10.Re, 25.70.Ef, 25.70.Mn, 27.20.+n

I. INTRODUCTION

There are few nuclei in nature more important than ^{12}C . Despite being one of the simplest, constituting only 12 nucleons, it has defied a detailed understanding. Moreover, it lies at the limits of state-of-the-art nuclear calculations such as the Green's-function Monte Carlo approach [1]. The first excited state at 4.4 MeV (2^+) can be understood as a collective excitation of the ground state [2], as can the 14.1 MeV excitation (4^+). The structure of the ground state has long been believed to be associated with a cluster state in which three α particles are arranged at the vertices of a triangle [3]. However, the ground state lies 7 MeV below the α -decay threshold, and hence, it is likely that the cluster structure is strongly suppressed [4]. Nevertheless, the symmetry persists; ^{12}C is oblate in the ground state. Above the α -decay threshold, enhancement of the cluster structure is possible. The 3^- state at 9.64 MeV may be associated with the threefold symmetry, which exists for a system associated with three α particles in an equilateral triangular arrangement, and recent measurements point to a 4^- state at 13.35 MeV [5,6] (previously assigned to be 2^- [7]) associated with a collective rotation around an axis perpendicular to the plane of the triangle.

Aside from the above understanding, the structure of the second excited state at 7.65 MeV, 0^+ , has yet to be determined. It is likely that it is associated with a pronounced cluster structure, but the arrangement of the clusters remains to be determined. The state was first proposed by Hoyle [8] as the gateway for the triple- α process, the mechanism by which ^{12}C is formed in stellar nucleosynthesis. Subsequently, the state was experimentally verified [9]. However, over 50 years later, the structure is not precisely determined. It has even been proposed to have a Bose condensate structure [10,11]. Recent measurements indicate that there may be a 2^+ excitation between 9 and 12 MeV [12–14], which may be associated with a collective rotational or vibrational excitation. However, the precise detail of the structure of ^{12}C in this important region remains to be fixed.

In the present paper we present evidence for a previously unknown state at 13.3 MeV that may be linked to the Hoyle state.

II. EXPERIMENTAL DETAILS

The present measurements were performed at the Notre Dame tandem facility. Beams of ^4He nuclei at energies between 22 and 30 MeV were incident on targets of 1 mg cm^{-2} ^9Be , 45 $\mu\text{g cm}^{-2}$ ^{12}C , and 2.5- μm -thick mylar. Beam intensities were typically 5 nA ($Q = 2^+$).

The reactions of particular interest here were $^{12}\text{C}(^4\text{He}, ^4\text{He} + ^4\text{He})^4\text{He}$ and $^9\text{Be}(^4\text{He}, ^4\text{He} + ^4\text{He} + ^4\text{He})n$, where in each case three α particles were detected. In order to detect such a complex, multiparticle, final state, an array of four 500- μm -thick, double-sided silicon strip detectors (DSSSDs) were employed. These were capable of stopping α -particle energies of up to 32 MeV and were operated with energy thresholds of 700 keV, with a typical energy resolution of 100 keV (full width at half maximum, FWHM). The DSSSDs each had a surface area of $5 \times 5 \text{ cm}^2$, which was subdivided into 16 horizontal and 16 vertical strips on the front and back faces, respectively. The detectors were arranged centered on the horizontal plane defined by the beam axis and the reaction chamber. For the measurements of the $^{12}\text{C}(^4\text{He}, ^4\text{He} + ^4\text{He} + ^4\text{He})^4\text{He}$ reaction, the detectors were placed at distances 9.4, 13.0, 13.0, and 10.3 cm from the target at angles 50.0° , 20.0° , -27.5° , and -55.0° , respectively (angles relative to the beam axis). Here the different signs of the angles indicate opposing sides of the beam axis. For the $^9\text{Be}(^4\text{He}, ^4\text{He} + ^4\text{He} + ^4\text{He})n$ measurements the distances were 6.8, 10.9, 10.7, and 6.5 cm at angles of 71.0° , 33.0° , -30.0° , and -69.0° , respectively.

The detectors were calibrated with α particles produced by ^{148}Gd (3.183 MeV) and ^{241}Am (5.486 MeV) sources and elastic scattering of the beam from a ^{208}Pb target.

III. ANALYSIS AND RESULTS

Given that the detectors had no explicit particle selection, reaction-channel identification was achieved via a reconstruction of the reaction kinematics. Events in which three of the four final-state particles were detected were processed. The detection system provides a determination of the energy and angle of each particle. Starting from an assumption

that each detected particle is an α particle, it is possible to reconstruct the momentum for each. The principle of momentum conservation then permits the momentum and energy of the fourth, unobserved, particle (recoil) to be reconstructed:

$$\underline{P}_{\text{rec}} = \underline{P}_{\text{beam}} - \sum_{i=1}^3 \underline{P}_{\alpha_i}, \quad (1)$$

$$E_{\text{rec}} = \frac{P_{\text{rec}}^2}{2m_{\text{rec}}}. \quad (2)$$

Here $\underline{P}_{\text{beam}}$ is the beam momentum, and \underline{P}_{α_i} are the calculated momenta of the three α particles. In the two reactions from the ${}^9\text{Be}$ and ${}^{12}\text{C}$ targets the recoil mass is assumed to be that of a neutron and α particle, respectively. The reaction Q value may then be calculated using

$$Q = E_{\text{rec}} + \sum_{i=1}^3 E_{\alpha_i} - E_{\text{beam}}, \quad (3)$$

where E_{α_i} is the energy of each detected particle and E_{beam} is the beam energy. The reaction of interest may then be identified from an associated Q -value spectrum. The Q -value spectra for the ${}^{12}\text{C}({}^4\text{He}, {}^4\text{He} + {}^4\text{He} + {}^4\text{He})$ and ${}^9\text{Be}({}^4\text{He}, {}^4\text{He} + {}^4\text{He} + {}^4\text{He})n$ reactions are shown in Figs. 1(b) and 1(a), respectively. In each case, there is only one peak that unambiguously identifies the reaction of interest. The Q value for the reaction proceeding from the ${}^{12}\text{C}$ target is -7.275 MeV and from the ${}^9\text{Be}$ target is -1.574 MeV. The data in Fig. 1(b) correspond to reactions reconstructed from the carbon component of the thick mylar target, which provided the highest statistics data set. The peaks in the spectra in Fig. 1 lie at -6.65 MeV and -0.89 MeV. The small discrepancy from the actual values may be attributed largely to the energy

loss of particles in the thick targets. The Q -value resolution for the α recoil was 1.1 MeV (FWHM), while in the case of the lighter neutron [Fig. 1(a)] it was 2.0 MeV (FWHM). The two reactions of interest were then selected via placing cuts centered on the two peaks in the Q -value spectra.

An additional level of selectivity that provides a restriction on possible final-state interactions was also imposed. Of the three detected α particles it is possible that two arose from the decay of ${}^8\text{Be}$. In particular, the identification of decays proceeding via the ${}^8\text{Be}$ ground state (which is unbound to α decay by 92 keV) is possible. Figure 1(c) shows the ${}^8\text{Be}$ decay spectrum reconstructed from pairs of the detected α particles for events falling within the peak in Fig. 1(b). The relative energy E_{rel} was calculated according to

$$E_{\text{rel}} = \frac{1}{2}\mu v_{\text{rel}}^2, \quad (4)$$

where μ is the reduced mass of a pair of α particles and v_{rel} is their relative velocity. The decays proceeding via the ${}^8\text{Be}$ ground state can be clearly identified with the peak at $E_{\text{rel}} = 92$ keV. Again, events within this peak were selected for further analysis.

A. The ${}^9\text{Be}({}^4\text{He}, {}^4\text{He} + {}^4\text{He} + {}^4\text{He})n$ reaction

The events associated with the ${}^9\text{Be}({}^4\text{He}, {}^4\text{He} + {}^4\text{He} + {}^4\text{He})n$ reaction were first selected by gating on the peak shown in Fig. 1(a). Second, it was demanded that two of the three detected α particles should arise from the decay of the ${}^8\text{Be}$ ground state. In this manner, the final state was constrained to be ${}^4\text{He} + {}^8\text{Be} + n$. There are a number of possible decay processes that can generate these three particles: (i) the α decay of ${}^{12}\text{C}$ states, (ii) neutron decay of states in ${}^9\text{Be}$, or (iii) neutron decay of states in ${}^5\text{He}$. In order to disentangle these possibilities a Dalitz plot has been constructed, as shown in Fig. 2. Here the reconstructed ${}^{12}\text{C}$ excitation energy (horizontal axis) is plotted versus the ${}^9\text{Be}$ excitation energy (vertical axis). The ${}^{12}\text{C}$ excitation energy was calculated from the measured energies and angles of the three detected α particles according to

$$E_x({}^{12}\text{C}) = \sum_i^3 E_i(\alpha) - E({}^{12}\text{C}) + 7.272, \quad (5)$$

where

$$E({}^{12}\text{C}) = \frac{[\sum_i^3 p_i(x)]^2 + [\sum_i^3 p_i(y)]^2 + [\sum_i^3 p_i(z)]^2}{2M_c}, \quad (6)$$

with $p_i(x)$, $p_i(y)$, and $p_i(z)$ being the x , y , and z components of the i th α particle and M_c being the mass of ${}^{12}\text{C}$. The excitation energy of the ${}^9\text{Be}$ nucleus was calculated by assuming the third α particle (not associated with the ${}^8\text{Be}$ decay) was the recoil in the ${}^9\text{Be}({}^4\text{He}, {}^9\text{Be}){}^4\text{He}$ reaction and subtracting the ground-state Q value (-10.739 MeV). Figure 2 reveals a series of vertical loci associated with ${}^{12}\text{C}$ states. In particular, the well-known 9.64-MeV (3^-), 10.84-MeV (1^-), and 14.08-MeV (4^+) states are populated. It should be noted that the selection of decays to the ${}^8\text{Be}$ ground state eliminates unnatural-parity

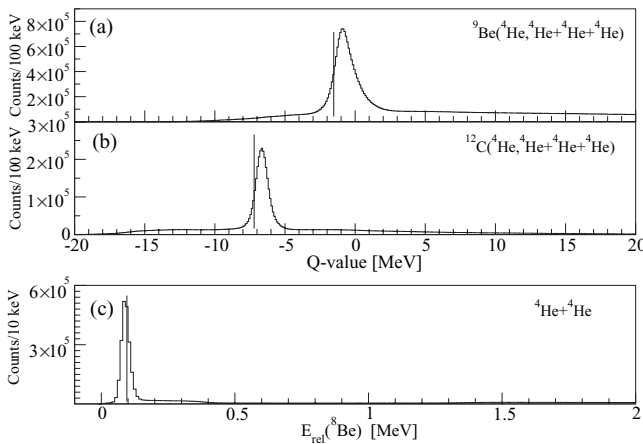


FIG. 1. (a) The Q -value spectrum for three detected particles assumed to proceed from the ${}^9\text{Be}({}^4\text{He}, {}^4\text{He} + {}^4\text{He} + {}^4\text{He})$ reaction. (b) The Q -value spectrum for three detected particles assumed to proceed from the ${}^{12}\text{C}({}^4\text{He}, {}^4\text{He} + {}^4\text{He} + {}^4\text{He})$ reaction. (c) Relative energy spectrum for two α particles. The peak associated with the decay from the ${}^8\text{Be}$ ground state is observed at 92 keV. The vertical lines indicate the expected energy of the three peaks. Discrepancies are due to uncertainties in the energy loss of the detected particles and the beam in the target.

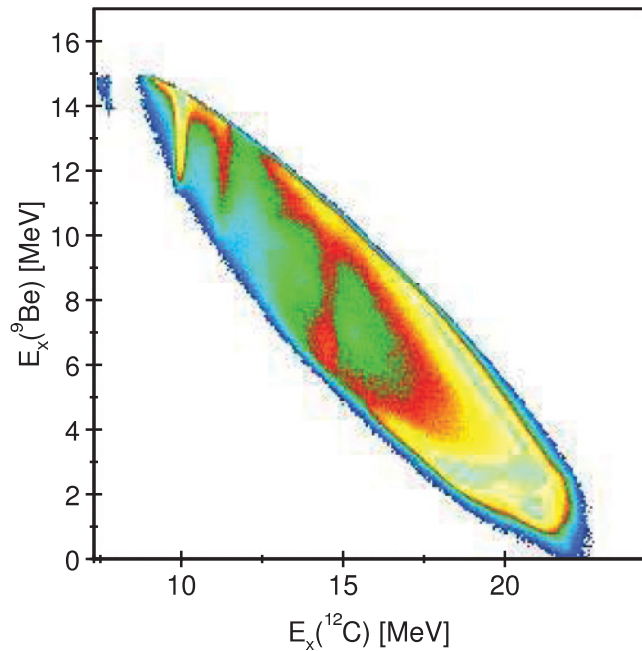


FIG. 2. (Color online) Dalitz plot for the $^9\text{Be}(^4\text{He}, ^4\text{He} + ^4\text{He} + ^4\text{He})n$ reaction measured at a beam energy of 22 MeV. The reconstructed ^{12}C excitation energy (horizontal axis) is plotted against the calculated ^9Be excitation energy. States associated with the decay of ^5He form diagonal loci.

states. Similarly, states in ^9Be are found that may be associated with the 1.68-MeV ($1/2^+$) state and most probably with the 2.43 MeV, $5/2^+$ state. Finally, there is a diagonal band with a gradient of -1 that would be associated with the decay of ^5He . In order to reveal the nature of the ^{12}C spectrum the data in Fig. 2 have been projected onto the horizontal axis, as shown in Fig. 3(a).

This latter spectrum clearly shows the three aforementioned states. However, there also appears to be an additional broad component close to 13 MeV. Such a component appears not to be associated with other final-state interactions, such as the decay of ^5He or ^9Be . However, if the broad structure were to be due to these other reaction processes, then a change of beam energy would result in a Dalitz plot in which the center-of-mass energy is increased and components move in energy relative to one another. Figure 3(a) also shows the projected spectra for a beam energy of 26 MeV. It is found that the two ^{12}C spectra below an excitation energy of 15 MeV are almost identical, particularly the 14.08-MeV 4^+ state and the broad structure. An alternate explanation for the additional strength close to 13 MeV could be that the gate on the ^8Be ground state is not entirely successful in excluding the unnatural-parity states. Figure 3(c) shows the ^{12}C excitation energy spectrum, which, rather than gating on the ^8Be ground state, excludes this state. This would permit unnatural-parity states decaying via $^8\text{Be}(2^+)$ to be observed. The resulting spectrum reveals peaks associated with the 11.83-MeV (2^-) and 12.71-MeV (1^+) states together with the 14.08-MeV, state which has a 83.0% ($\pm 0.4\%$) decay branch [15] to the $^8\text{Be}(2^+)$ state. It is clear that the structure in this latter spectrum is not

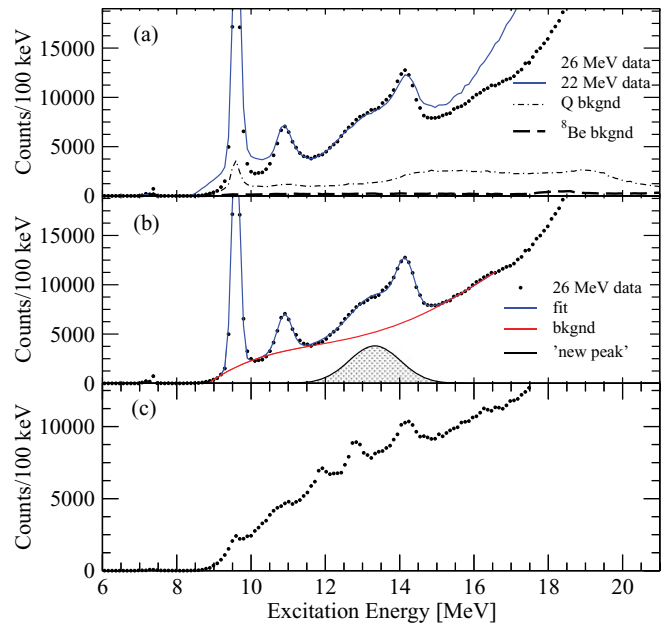


FIG. 3. (Color online) Carbon-12 excitation energy spectra. (a) Projection of the data in Fig. 2 onto the horizontal axis (blue solid line). The spectrum corresponding to measurements at 26 MeV is shown by the dots. The backgrounds obtained by gating above the ^8Be peak (thick dashed line) and both above and below the Q -value peak (dot-dashed line) are both illustrated. (b) Fit to the 26-MeV data, given by the blue solid line. The polynomial background (red line) and line shape for the new peak (shaded area) is shown (see text for details). (c) Excitation energy spectrum for events not proceeding via the decay to the ^8Be ground state.

replicated in Fig. 3(a) and hence is not the origin of the broad structure.

Alternatively, possible contaminants in the ^{12}C excitation energy spectrum may arise from backgrounds lying beneath the peaks in Figs. 1(a) and 1(c). Figure 3(a) shows the ^{12}C excitation spectra for (i) the ^8Be gate moved up in energy by 180 keV (labeled ^8Be bkgnd) and (ii) the average background from moving the gate on the Q -value spectrum to both above and below the peak in the spectrum in Fig. 1(c) (labeled Q bkgnd). It is clear that the contribution from the first of these is negligible, although the corresponding ^9Be excitation energy spectrum does emphasize the 2.43-MeV ($5/2^+$) state, which is known to preferentially decay to the low-energy tail of the $^8\text{Be}(2^+)$ state [16]. The background from the Q -value spectrum is more significant. The 3^- state is evident, which is believed to originate from the $^{16}\text{O}(^4\text{He}, ^4\text{He} + ^4\text{He} + ^4\text{He})^8\text{Be}$ reaction, arising from the ^{16}O contaminant arising from oxidation of the beryllium target. This background was reconstructed by averaging the background spectra from above and below the peak found in Fig. 1(a). It does not reveal any evidence for the broad structure identified above. Figure 3(b) shows the 26-MeV spectrum that appears in Fig. 3(a), but fitted with four peaks and a background component. The background has been selected to be a fifth-order polynomial with peaks associated with the known states at 9.64, 10.84, and 14.08 MeV. These have been modeled by Gaussian line shapes with 260-, 460-, and 560-keV resolutions (FWHM),

respectively; it is known that the excitation energy resolution in the invariant mass technique increases as the square root of the energy above the decay threshold. The fourth and previously unrecorded state was again modeled by a Gaussian line shape centered at 13.3 MeV with a FWHM of 1.7 MeV [as shown by the shaded region in Fig. 3(b)]. Given the uncertainty in the shape of the background, the uncertainty on the width and centroid is of the order of 200 keV in both cases.

Although the measurements at both energies reveal the new structure at exactly the same energy and the Dalitz plot shown in Fig. 2 appears to show a vertical locus associated with the structure, further verification of its association with the decay of ^{12}C would be desirable. To this end, a similar analysis of the $^{12}\text{C}(^4\text{He}, ^4\text{He} + ^4\text{He} + ^4\text{He})\alpha$ reaction is presented below.

B. The $^{12}\text{C}(^4\text{He}, ^4\text{He} + ^4\text{He} + ^4\text{He})\alpha$ reaction

In order to select the reaction of interest the peak observed in Fig. 1(b) was selected, and subsequently, events in which two of the α particles were produced from the decay of ^8Be were chosen by gating on the peak in the ^8Be relative energy spectrum [Fig. 1(c)]. As with the analysis of the reactions from the ^9Be target, there are three possible ways the final state can arise: (i) the three detected α particles were produced from the decay of states in ^{12}C , (ii) the ^8Be and the undetected α particle were associated with the decay of ^{12}C , or (iii) the reaction was $^{12}\text{C}(\alpha, ^8\text{Be})^8\text{Be}$. In the last case the “recoil” ^8Be nucleus could be in a ground or excited state. The corresponding Dalitz plot for a beam energy of 30 MeV is shown in Fig. 4.

Here the excitation energy in ^{12}C calculated from the three detected α particles (horizontal axis) is plotted versus that calculated assuming the unobserved α particle was produced from the decay of ^{12}C (vertical axis). In the latter case, it was assumed that the third detected α particle, i.e., the one not associated with the decay of ^8Be , was the recoil in the $^{12}\text{C}(^4\text{He}, ^4\text{He} + ^4\text{He} + ^4\text{He})\alpha$ reaction. Here the three detected α particles are labeled 1, 2, and 3, with particles 1 and 2 being from the decay of ^8Be . The fourth, undetected α particle is labeled 4. The final state then consists of $^8\text{Be} + \alpha_3 + \alpha_4$. The excitation energy on the horizontal axis of Fig. 4 was calculated using equations (5) and (6). The excitation energy on the vertical axis was calculated from the measurement of the momentum of α_3 while assuming the other particles to arise from the decay of ^{12}C and momentum conservation and two-body kinematics:

$$E_x(^{12}\text{C}) = E_{\text{beam}} - [E_3(\alpha) + E_{\text{rec}}], \quad (7)$$

where

$$E_{\text{rec}} = \frac{p_3(x)^2 + p_3(y)^2 + [p_{\text{beam}} - p_3(z)]^2}{2 \times 12}, \quad (8)$$

with p_{beam} being the beam momentum. In this instance, the reconstructed ^{12}C excitation energy resolution is inferior (FWHM = 600 keV) at lower excitation energies than the invariant mass approach, but it is energy independent and thus close to equivalent at higher excitation energies. A very similar spectrum of states is observed in both the horizontal

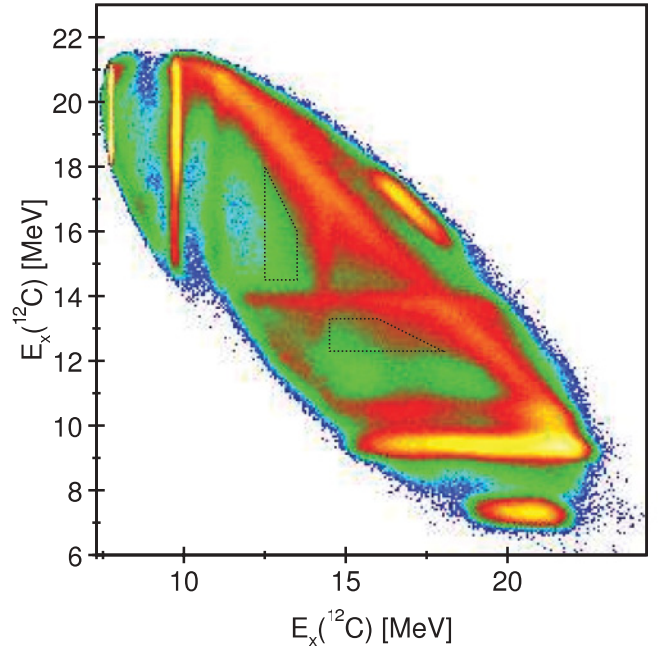


FIG. 4. (Color online) Dalitz plot for the $^{12}\text{C}(^4\text{He}, ^4\text{He} + ^4\text{He} + ^4\text{He})\alpha$ reaction measured at a beam energy of 30 MeV. The ^{12}C excitation energy reconstructed from the three detected α particles is plotted on the horizontal axis. The vertical axis corresponds to the ^{12}C excitation energy calculated assuming that, in addition to the ^4He nuclei detected from the ground state decay of ^8Be , the third detected α particle is the recoil in the above reaction. States associated with the decay of ^8Be form diagonal loci. The dotted boxes show the region selected for the angular correlation measurements of the 13.3-MeV peak, which is shown in Fig. 7.

and vertical directions and is also similar to that seen in Fig. 2. The loci running diagonally (with a gradient of -1) correspond to states in ^8Be ; the ground state is seen at the highest side of the Dalitz region. Similar evidence for the excitation of the ^8Be 2^+ and 4^+ states can be found for excitations at 3.0 and 11.3 MeV, respectively. In both the horizontal and vertical versions of the ^{12}C spectrum a broad band can be found just below the 14.08-MeV excitation.

The Dalitz plot shown in Fig. 4 is projected vertically and horizontally, as shown in Figs. 5(a) and 5(b), respectively. As with the ^9Be target, the states observed are the 9.64-, 10.84-, and 14.08-MeV states. In addition, there is some contribution from the 7.65-MeV state, which was not strongly observed with the ^9Be target due to the experimental acceptance. Just as before, there is an additional contribution that lies below the 14.08-MeV state, which appears in both spectra. Figure 5(c) shows the excitation energy spectrum for the condition when a pair of the detected α particles was not produced from the decay of the ^8Be ground state. This would include decays proceeding to ^8Be excited states. Once again, the structure of the spectra in Figs. 5(a) and 5(b) does not follow that in Fig. 5(c). These spectra have been fitted in an identical fashion to Fig. 3(b), i.e., a fifth-order polynomial background and peaks at 9.64-, 10.84-, 14.08-, and 13.3-MeV. The spectra are consistent with the same line shape for the new component.

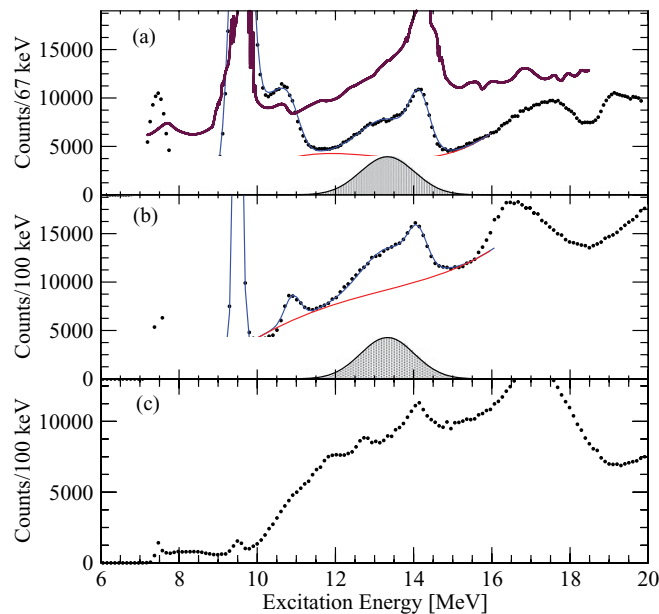


FIG. 5. (Color online) Carbon-12 excitation energy spectra. (a) Projection of the data in Fig. 4 onto the vertical axis (dots). The fit to the data (blue line) is shown together with the polynomial background (red line) and the proposed peak (shaded region). The vertically displaced spectrum is extracted from the previously reported $^9\text{Be}(^4\text{He},^{12}\text{C})$ measurements (see Fig. 1 in Ref. [20]). (b) Projection of the data in Fig. 4 onto the horizontal axis (dots). The fit to the data (blue line) is shown together with the polynomial background (red line) and the proposed peak (shaded region). (c) Excitation energy spectrum for events not proceeding via the decay to the ^8Be ground state.

It is clear that, for the two reactions measured here, there is a component in the spectrum that cannot be accounted for by previously known states. It is possible that it arises from a single broad resonance with a width of 1.7(0.2) MeV at 13.3(0.2) MeV or that it is several unresolved states.

IV. ANGULAR CORRELATIONS

In order to gain an insight into the nature of the proposed new state in ^{12}C we have examined the distribution pattern of α particles in the decay. Formally, this technique is called angular correlations. This method may most simply be applied when the initial- and final-state particles are all spin zero, and hence, it has been applied to the ^{12}C target data only. In this case a model-independent analysis is possible [17]. In the correlation analysis, it is necessary to define two angles: θ^* and ψ . The angle θ^* defines the center-of-mass emission angle of the ^{12}C nucleus in the $^{12}\text{C}(\alpha, ^{12}\text{C}^*)\alpha$ reaction. Then ψ defines the angle of emission of the first α particle from the decay of the excited ^{12}C nucleus, within the ^{12}C center-of-mass frame. Both angles are measured with respect to the beam axis. Using the Dalitz plot in Fig. 4, it is possible to place event selection windows around the various loci that determine both the excitation energy and the origin of the particles detected. Using this procedure, the angular correlation plots shown in Figs. 6(a)–6(d) were created for the 0^+ , 7.65-MeV; 1^- ,

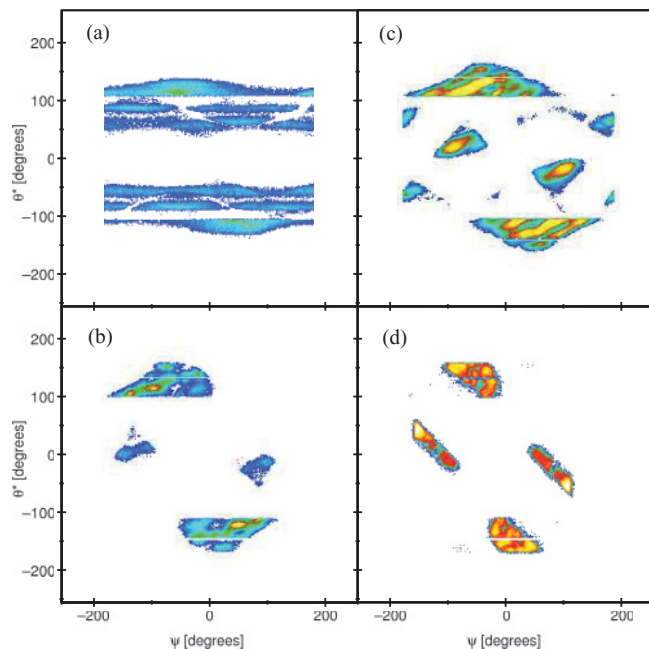


FIG. 6. (Color online) Angular correlation plots for states of known spin and parity. (a) 7.65 MeV, 0^+ , (b) 10.84 MeV, 1^- , (c) 9.64 MeV, 3^- , and (d) 14.08 MeV, 4^+ .

10.84-MeV; 3^- , 9.64-MeV; and 4^+ , 14.08-MeV states, respectively. These spectra illustrate the key features of angular correlations. The correlation structure in the θ^* - ψ plane is governed, to first order, by

$$W(\theta^*, \psi) \propto |P_J[\cos(\psi + \Delta\psi)]|^2, \quad (9)$$

where a small change in ψ , $\Delta\psi$, is related to a small change in θ^* , $\Delta\theta^*$, via

$$\Delta\psi = \Delta\theta^* \frac{l_g - J}{J}, \quad (10)$$

where J is the spin of the state and l_g is the dominant entrance channel angular momentum, usually called the grazing angular momentum [17]. P_J is a Legendre polynomial of order J . Hence, at $\theta^* = 0$, the correlation pattern should follow an intensity given by $|P_J[\cos(\psi)]|^2$. Away from 0° , the periodicity remains the same, but there is a shift in phase that is roughly linear with the change in angle $\Delta\theta^*$. This gives rise to a series of sloping ridges. The gradient of the ridges $\Delta\theta^*/\Delta\psi$ is given by $J/(l_g - J)$. Hence, both the periodicity and the gradient may be used to extract the spin of the ^{12}C state decaying to $^8\text{Be}_{\text{gs}} + \alpha$. For a spin-zero state, as with the state at 7.65 MeV, the gradient should be zero. Figure 6(a) shows a series of horizontal bands cut by the experimental acceptance. The correlations for the 1^- and 3^- states are shown in Figs. 6(b) and 6(c), respectively. The ridges referred to above can most clearly be seen for the 3^- state. In order to characterize the periodicity, the data are typically projected parallel to the ridges onto the ψ axis. The angle at which the data are projected then provides one determination of the spin of the state. For the $^{12}\text{C}(^4\text{He}, ^4\text{He})$ reaction at 30 MeV, we estimate that the grazing angular momentum is $9\hbar$. The optimum angles for the projection of the data for the 1^- , 3^- , and 4^+ states

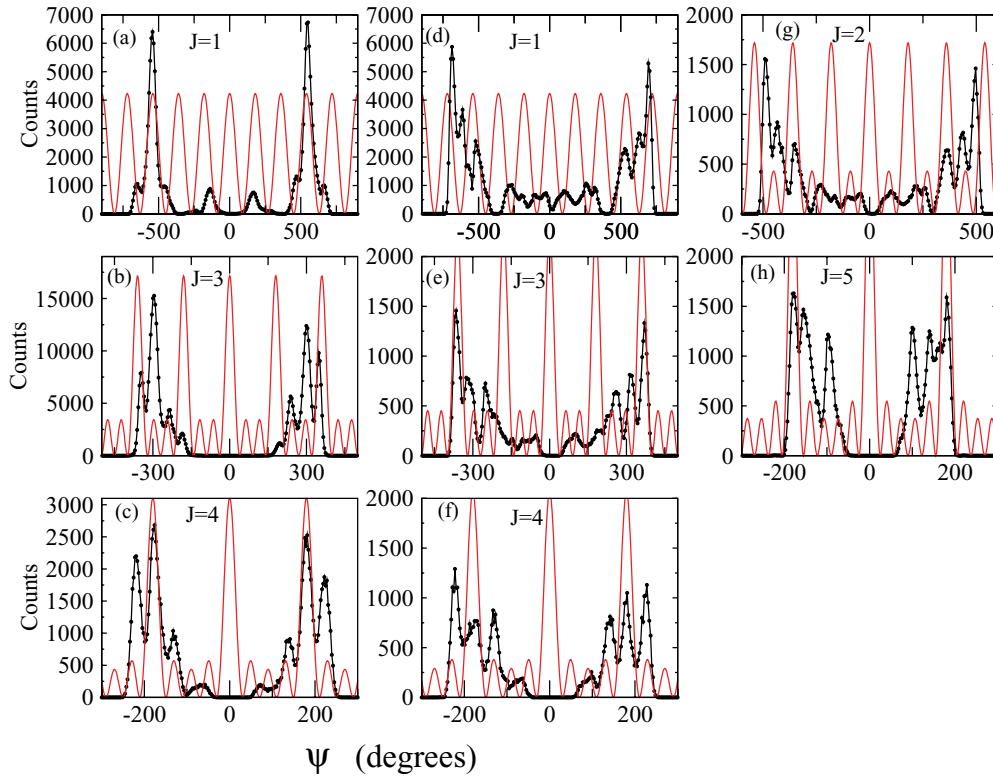


FIG. 7. (Color online) Angular correlations projected onto the ψ axis (dots) compared with $P_J[\cos(\psi)]^2$ functions. (a) 10.84 MeV, 1^- ; red line shows $P_1[\cos(\psi)]^2$. (b) 9.64 MeV, 3^- ; red line shows $P_3[\cos(\psi)]^2$. (c) 14.08 MeV, 4^+ ; red line shows $P_4[\cos(\psi)]^2$. (d), (e), and (f) The corresponding data associated with the 13.3-MeV peak projected at the same angles as in (a), (b), and (c), respectively. The Legendre polynomials shown (red lines) are (d) $P_1[\cos(\psi)]^2$, (e) $P_3[\cos(\psi)]^2$, and (f) $P_4[\cos(\psi)]^2$. (g) and (h) The data for the 13.3-MeV peak projected at angles for states of spin 2 and 5, respectively; the red lines show (g) $P_2[\cos(\psi)]^2$ and (h) $P_5[\cos(\psi)]^2$.

was found to be $\Delta\theta^*/\Delta\psi = 14^\circ$, 27° , and 44° , respectively, which would correspond to 5, 9, and 8 \hbar , which is reasonably close to the calculated value. The corresponding projections are shown in Figs. 7(a), 7(b), and 7(c), respectively. The data are compared with Legendre polynomials of the appropriate order in each case. The reproduction of the periodicity of the oscillations found in the data is reasonably good, confirming the robustness of the technique to extract the spins. It should be noted that the Legendre polynomials shown in Fig. 7 have not been fed through the experimental acceptance as they are used only to illustrate the periodicity. In order to reproduce the amplitudes of the oscillations a full reaction model calculation predicting the variation of the m substates as a function of scattering angle θ^* would be required, which is beyond the scope of the current work.

In order to gain an insight into the possible spin of the broad peak found in the ^{12}C excitation energy spectrum the corresponding correlations were analyzed. In order to select the appropriate events, two windows were placed to the low-energy sides of the two 14.08-MeV loci in Fig. 4, making sure that possible contributions from the ^{12}C and ^8Be 4^+ states were excluded. The correlation data were then projected at the optimum angles found for the 1^- , 3^- , and 4^+ states. These projections are shown in Figs. 7(d), 7(e), and 7(f). Of these three possibilities, the data appear to agree best with the periodicity of the Legendre polynomial for the $J^\pi = 4^+$ case.

Figures 7(g) and 7(h) correspond to projections at 20° and 53° and are compared with Legendre polynomials of orders 2 and 5, respectively. Due to the rather constrained cut placed on the Dalitz plot of Fig. 4, this analysis does not yield an unambiguous result for the spin of a state associated with the broad bump. However, they would appear to exclude $J^\pi = 1^-$ and 2^+ , and the striking similarity between the periodicity of the oscillations found in Figs. 7(c) and 7(h) would favor $J^\pi = 4^+$.

V. DISCUSSION

The present measurements indicate the presence of a new state in ^{12}C at 13.3(0.2) MeV with a width of 1.7(0.2) MeV. Given that the line shape is similar for the two different beam energies with the ^9Be target and the ^{12}C target data, then it is assumed that the peak corresponds to a single state rather than a collection of unresolved states. The state must have natural parity, $(-1)^J$, as the decay proceeds to the $^4\text{He} + ^8\text{Be}$ decay channel that contains exclusively spin-zero nuclei. The present measurements would indicate $J^\pi = 4^+$, although other spins cannot be excluded.

There are several measurements that previously probed the structure of ^{12}C in the present region. The measurement of the $^{12}\text{C}(^{12}\text{C},3\alpha)$ reaction [6] is the closest to those presented here. In that case, the α decay to the ^8Be ground and excited

states was separately analyzed. In the decay to the ground state the 7.65-MeV (0^+), 9.64-MeV (3^-), 10.84-MeV (1^-), and 14.08-MeV (4^+) states were clearly identified. The main focus was the analysis of the decay of the unnatural-parity states. No strong feature was observed close to 13.3 MeV (although a background contribution peaking close to 12.5 MeV was required). Angular correlation studies appeared to indicate dominant $L = 1$ and 3 strength between the 10.84- and 14.08-MeV peaks, with the $L = 3$ strength being located close to 12.5 MeV. No clear peaks were identified in this region.

Measurements of the $^{11}\text{B}(^3\text{He},3\alpha)$ reaction have recently been reported [5]. Again, the decay channel selection was possible, and in the current region, no feature close to 13.3 MeV was observed that could be associated with natural-parity states. Indeed, predominantly, unnatural-parity states were strongly populated in this reaction.

Analysis of the β decay of ^{12}B and ^{12}N to ^{12}C followed by the detection of three α particles has been measured by the Aarhus group on several occasions [12,18]. Such studies are sensitive to states with spin and parity 0^+ , 1^+ , and 2^+ . The most recent of these measurements indicates that a broad 2^+ state exists between 10.5 and 12 MeV and that a further 2^+ state lies close to 16.5 MeV, with no indication of a 0^+ or 2^+ state close to 13.3 MeV.

One earlier measurement of the $^9\text{Be}(\alpha,n)$ reaction was found at an incident energy of 35 MeV, close to the present energy [19]; this result, though unpublished, is presented in Fig. 1 of Ref. [20] [and is shown in Fig. 5(a)]. The measurement was made at a laboratory angle of 32° and shows that the unnatural-parity states are not strongly populated as in the present case. The 14.08-MeV, 4^+ state is clearly observed as is an unresolved broad structure extending to lower excitation energies. This feature appears to be identical to the one observed in the present measurements.

Hence, if the broad peak reported in the current measurements corresponds to a state in ^{12}C , it appears not to have been previously reported but is also observed in an unpublished measurement of the $^9\text{Be}(\alpha,n)$ reaction [19]. There may be two reasons that it has not been more widely observed; first, the decay channel selectivity ($^8\text{Be}_{gs}$) is important in suppressing the unnatural-parity states in this region, and second, the

reaction mechanism may play a role. In the case of the $^9\text{Be} + \alpha$ reaction, ^9Be has a well-developed $2\alpha + n$ cluster structure in the ground state. The “fusion” with an α particle would then lead to states with a $3\alpha + n$ structure from which the neutron is evaporated. Similarly, the $^{12}\text{C} + \alpha$ reaction could lead to the formation of $4p - 4h$ cluster states in ^{12}C . The other reactions discussed above would appear not to strongly populate such excitations.

The angular correlation measurements presented here do not provide a definitive measurement of the spin of the state. However, it is clear that it should possess natural parity, i.e., 0^+ , 1^- , 2^+ , etc. The data in Fig. 7 favor $J^\pi = 4^+$, although other spins cannot be excluded. Based on the β -decay measurements, 2^+ can be excluded, and then after 4^+ , the next most likely possibility would be 5^- .

If the state does have 4^+ character, then it is most likely associated with a collective excitation of the 7.65 MeV, 0^+ , Hoyle state. Using a rotational model and an excitation energy of 13.3 MeV, it is possible to interpolate the energy of a possible 2^+ state. This approach would indicate a 2^+ excitation at 9.35(0.06) MeV. It should be observed that this is very close to that proposed in Refs. [13,14]. Measurements of the $^{12}\text{C}(\alpha,\alpha')$ [13] and $^{12}\text{C}(p,p')$ [14] reactions indicate a 2^+ state close to 9.6(0.2) MeV [$\Gamma = 0.6(0.2)$ MeV]. Given this close coincidence, it is possible that a collective structure associated with the 7.65-MeV state has been observed with the 2^+ and 4^+ members at 9.6 and 13.3 MeV.

VI. CONCLUSION

The current measurements of the $^9\text{Be}(^4\text{He},^{12}\text{C}^*)n$ and $^{12}\text{C}(^4\text{He},^{12}\text{C}^*)^4\text{He}$ reactions reveal evidence for a resonance at 13.3(0.2) MeV with a width of 1.7(0.2) MeV. Angular correlation measurements from the ^{12}C target measurements do not provide an unambiguous spin determination but indicate that the state has a spin and parity $J^\pi = 4^+$. Unambiguously, the state must have natural parity. It is suggested that this state could be a collective excitation of the Hoyle state, a description that is consistent with earlier reports of a 2^+ state close to 9.6 MeV.

-
- [1] R. B. Wiringa, S. C. Pieper, J. Carlson, and V. R. Pandharipande, *Phys. Rev. C* **62**, 014001 (2000).
 [2] R. Bijker and F. Iachello, *Phys. Rev. C* **61**, 067305 (2000).
 [3] L. R. Hafstad and E. Teller, *Phys. Rev.* **54**, 681 (1938).
 [4] K. Ikeda *et al.*, *Prog. Theor. Phys. Suppl.*, Extra Number, 464 (1968).
 [5] O. S. Kirsebom *et al.*, *Phys. Rev. C* **81**, 064313 (2010).
 [6] M. Freer *et al.*, *Phys. Rev. C* **76**, 034320 (2007).
 [7] F. Ajzenberg-Selove, *Nucl. Phys. A* **506**, 1 (1990).
 [8] F. Hoyle, *Astrophys. J. Suppl. Ser.* **1**, 121 (1954).
 [9] C. W. Cook *et al.*, *Phys. Rev.* **107**, 508 (1957).
 [10] Y. Funaki *et al.*, *Eur. Phys. J. A* **28**, 259 (2006).
 [11] A. Tohsaki, H. Horiuchi, P. Schuck, and G. Röpke, *Phys. Rev. Lett.* **87**, 192501 (2001).
 [12] S. Hyldegaard *et al.*, *Phys. Rev. C* **81**, 024303 (2010).
 [13] M. Itoh *et al.*, *Nucl. Phys. A* **738**, 268 (2004).
 [14] M. Freer *et al.*, *Phys. Rev. C* **80**, 041303 (2009).
 [15] D. D. Caussyn, G. L. Gentry, J. A. Liendo, N. R. Fletcher, and J. F. Mateja, *Phys. Rev. C* **43**, 205 (1991).
 [16] N. I. Ashwood *et al.*, *Phys. Rev. C* **72**, 024314 (2005).
 [17] M. Freer, *Nucl. Instrum. Methods Phys. Res., Sect. A* **383**, 463 (1996).
 [18] H. O. U. Fynbo *et al.*, *Nature (London)* **433**, 136 (2005).
 [19] J. J. Hamill, D. A. Lind, R. J. Peterson, R. S. Raymond, P. A. Smith, M. Yasue, and C. D. Zafiratos, *Bull. Am. Phys. Soc.* **76**, 579 (1981).
 [20] X. Aslanoglou and K. W. Kemper, *Phys. Rev. C* **34**, 1649 (1986)